Superficial and deep changes of histology, texture and particle size distribution in broiler wooden breast muscle during refrigerated storage

Francesca Soglia,[*] Jingxian Gao,[†] Maurizio Mazzoni,[‡] Eero Puolanne,[†] Claudio Cavani,[*] Massimiliano Petracci,[*] and Per Ertbjerg[†,1]

[*]*Department of Agricultural and Food Sciences, Alma Mater Studiorum - University of Bologna, 47521 Cesena, Italy;* [†]*Department of Food and Environmental Sciences, FI-00014 University of Helsinki, Helsinki, Finland; and* [‡]*Department of Veterinary Medical Sciences, Alma Mater Studiorum - University of Bologna, 40064 Ozzano dell'Emilia (BO), Italy*

ABSTRACT Recently the poultry industry faced an emerging muscle abnormality termed wooden breast (WB), the prevalence of which has dramatically increased in the past few years. Considering the incomplete knowledge concerning this condition and the lack of information on possible variations due to the intra-fillet sampling locations (superficial *vs.* deep position) and aging of the samples, this study aimed at investigating the effect of 7-d storage of broiler breast muscles on histology, texture, and particle size distribution, evaluating whether the sampling position exerts a relevant role in determining the main features of WB. With regard to the histological observations, severe myodegeneration accompanied by accumulation of connective tissue was observed within the WB cases, irrespective of the intra-fillet sampling position. No changes in the histological traits took place during the aging in either the normal or the WB samples. As to textural traits, although a progressive tenderization process took place during storage ($P \leq 0.001$), the differences among the groups were mainly detected when raw meat rather than cooked was analyzed, with the WB samples exhibiting the highest ($P \leq 0.001$) 80% compression values. In spite of the increased amount of connective tissue components in the WB cases, their thermally labile cross-links will account for the similar compression and shear-force values as normal breast cases when measured on cooked samples. Similarly, the enlargement of extracellular matrix and fibrosis might contribute in explaining the different fragmentation patterns observed between the superficial and the deep layer in the WB samples, with the superficial part exhibiting a higher amount of larger particles and an increase in particles with larger size during storage, compared to normal breasts.

Key words: Broiler, Wooden Breast, Histology, Texture, Particle size

2017 Poultry Science 0:1–8
http://dx.doi.org/10.3382/ps/pex115

INTRODUCTION

The poultry industry has in recent years faced an increasing demand of poultry meat as a consequence of its nutritional profile (low fat and high-value protein content coupled with a balanced n-6/n-3 PUFA ratio), suitability for further processing and lower price in comparison with red meats (Petracci et al., 2013). However, the selection of fast-growing broilers may have been a reason for an increased incidence of several muscle abnormalities such as WB (Petracci et al., 2015). The WB condition was first described by Sihvo et al. (2014) as the appearance of hardened, out-bulging and pale areas (often associated with white striations) in the surface of the *Pectoralis major* muscle. The WB muscles clearly exhibit severe histological lesions, including fiber degeneration and regeneration, fibrosis, and lipidosis (Sihvo et al., 2014; De Brot et al., 2016; Soglia et al., 2016) similar to other muscle dystrophies (Velleman, 2015). The incidence of WB in broilers is higher in males than in females and can reach 16% (Trocino et al., 2015) or even higher. Although the WB fillets are normally downgraded by the poultry industries, the water-holding capacity and textural properties of the processed products might be severely impaired by the inclusion of WB meat within the formulation (Mudalal et al., 2015; Petracci et al., 2015; Soglia et al., 2016).

When muscle is homogenized, it will give rise to a specific fragmentation pattern that reflects its original structure. A previous study performed on avian muscles revealed that the fragmentation following homogenization of the muscle tissue resulted in larger pieces in dystrophic cases compared to normal (Feit and Domke, 1982). This variation in muscle fragmentation observed within the dystrophic samples might either be due to an

Received August 3, 2016.
Accepted April 25, 2017.
[1]Corresponding author: per.ertbjerg@helsinki.fi

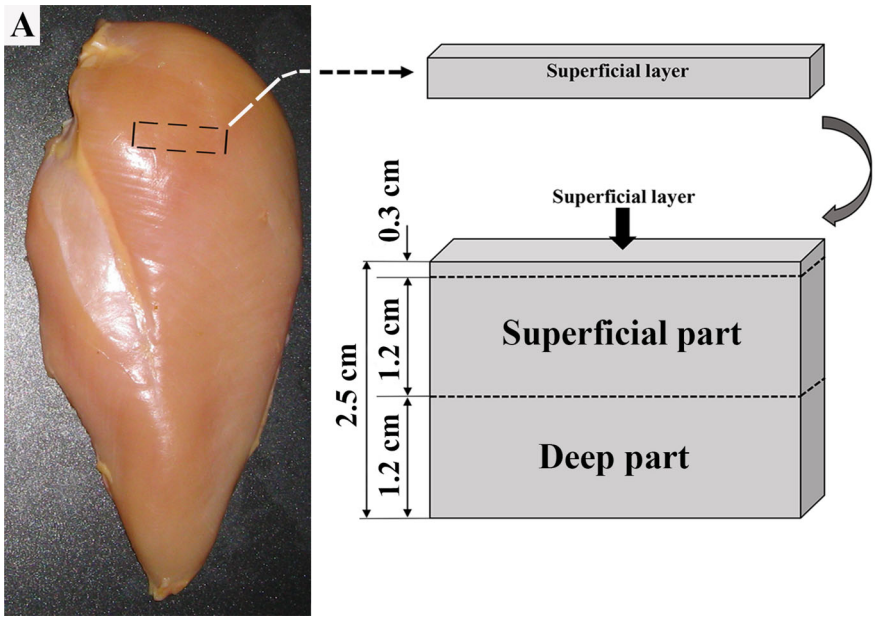

Figure 1. Representation of the sampling site and respective procedures carried out to subdividing a portion of the *Pectoralis major* muscle in the superficial and deep part.

overall reorganization of tissue architecture or to a different post-mortem degradation of structural proteins. Protein degradation occurring in post-mortem muscles was previously measured by the Myofibril Fragmentation Index (Olson et al., 1976), reflecting the degradation of key structural proteins in the I-band of the sarcomere (Taylor et al., 1995). However, the main disadvantage of this method is the time-consuming steps necessary to prepare the sample. In previous studies performed by Lametsch et al. (2007) and Karumendu et al. (2009), multi-angle light scattering generated by particles of different sizes was used, instead of the traditional turbidity method, to estimate myofibril fragmentation in porcine and ovine *Longissimus thoracis* and *lumborum* muscles, with the major advantage being the simple sample preparation required to perform the analysis. Laser diffraction is a widely used technique to describe the particle size distribution for materials in which the particles range in size from nanometers to millimeters. According to the Mie theory of light scattering, a laser beam passing through a homogenized-dispersed sample is scattered with an angular variation that is dependent on the particle size: small and high scattering angles result from large and small particles, respectively (Malvern, 2015). Moreover, since particle size can be measured on a meat homogenate without any further sample preparation, the analyzing time can be reduced up to 4 times (Lametsch et al., 2007).

Considering the very limited information available on the possible variation due to the intra-fillet sampling locations and the behaviour during refrigerated storage of WB fillets, this study aimed at investigating the effect of a 7-d storage of broiler breast fillets on histology, texture. and particle size distribution within the superficial and the deep layers of the *Pectoralis major* muscles.

MATERIALS AND METHODS

Histology

The histological evaluation was performed on a total of 18 *Pectoralis major* muscles (9 normal breast (**NB**) and 9 WB cases) selected at 3 h post mortem, from 35-day-old broilers (Ross 308, males, having an average weight of 2.5 kg), in the deboning area of a commercial processing plant. After being stored for 10, 72, and 168 h post mortem, each fillet was sampled and cut in order to separate the superficial from the deep layer according to the sampling protocol summarized in Figure 1. In detail, the "superficial layer" was defined from about 0.2 cm to 1.2 cm below the breast muscle surface. Besides, the "deep layer" was defined from about 1.5 cm to 2.5 cm below the breast muscle surface, few millimeters away from the superficial one. Then, both the superficial and the deep layer of each fillet was immediately fixed in a 10% buffered formalin solution for 24 h at room temperature. Specimens were oriented for transverse fiber sectioning, dehydrated in a graded series of ethanol, and embedded in paraffin. From each sample, 8 transverse sections (6 μm thick) were obtained, mounted on polylysine-coated slides and stained with Masson's trichrome. The presence of abnormal fibers (fibers exhibiting hyaline degeneration and damaged fibers with round profile) was assessed in 10 primary myofiber fascicles (PMF) randomly selected from the 8 transverse sections and the levels of myodegeneration graded (score F1, F2 and F3,

respectively) according to the same criteria adopted in previous studies (Mazzoni et al., 2015; Sihvo et al., 2017; Soglia et al., 2016).

Texture and Particle Size Analysis

Sample Collection A total of 180 *Pectoralis major* muscles were randomly selected at 3 h post mortem, from 37- to 38-day-old male broilers Ross 508, in the deboning area of a commercial processing plant. The samples were classified by 2 experienced people by manual palpation as Normal (NB) and WB (WB) according to the criteria of Sihvo et al. (2014). After trimming the muscles from visible fat and connective tissue they were packed into loose polyethylene bags and stored at $4 \pm 1^{\circ}$C until 10, 24, 72, 120, and 168 h post mortem. At each sampling time, 18 NB and 18 WB fillets were cut in order to separate the superficial from the deep layer and used to assess texture (on both raw and cooked meat), measure the shear force of cooked meat and perform particle size analysis.

Texture Analysis At each sampling time, compression force and Allo-Kramer shear test were performed on both the superficial and the deep layer of 18 NB and 18 WB fillets. The compression test was performed in triplicates on both the superficial and the deep layer of a total of 12 NB and 12 WB fillets: 6 raw and 6 vacuum-packaged and cooked (core temperature 75°C) samples. The test was performed on a $2 \times 1 \times 1$ cm sample by using a TA-XT2i Texture Analyser (Stable Micro Systems Ltd, Godalming, Surrey, UK) set to compress the sample in a longitudinal conformation applying the force perpendicular to the muscle fibers (Lepetit and Culioli, 1994) using a modified compression device (Campo et al., 2000). The sample was compressed to 95% of its initial height with a speed of 50 mm/min. Then, the forces recorded after compressing the sample at 40 and 80% of its initial height were extracted in order to estimate the contribution given by the myofibrils and the connective tissue, respectively (Lepetit and Culioli, 1994; Campo et al., 2000).

Allo-Kramer shear test was performed at each sampling time on both the superficial and the deep layer of 6 NB and 6 WB cooked fillets by using an Instron Model 6625 (Instron Co., Canton, MA) equipped with an Allo-Kramer shear cell and a 5 kN load cell. According to Liu et al. (2014), a total of six ($20 \times 20 \times 6$ mm) sub-samples, 3 from the superficial and 3 from the deep layer, were cut from each fillet and sheared with a test speed of 40 mm/min. The results were expressed as N/g of sample.

Particle Size Analysis The particle size distribution was analyzed following the procedure proposed by Lametsch et al. (2007) with slight modifications. Each sample (2.5 g) was homogenized in 20 mL of cold phosphate buffer (100 mM KCl, 20 mM Potassium Phosphate (pH 7.0), 1 mM EDTA, 1 mM $MgCl_2$) at 13,500 rpm using an Ultra-Turrax T25 basic (IKA-Werke, Staufen, Germany). Particle size was measured using a Malvern Mastersizer 3000 (Malvern Instruments Ltd, Worchester, UK). The instrument measures the particle size distribution based on the angular variation in intensity of light scattered as a laser beam passes through a wet dispersed particulate sample. According to the concept of the equivalent sphere, particle size is defined by the diameter of an equivalent sphere having the same volume as the actual particle. The instrument was connected to a wet dispersion unit containing water and the sample was added drop-wise to the unit while stirring before measuring. The refractive index was set to 1.46, absorption coefficient to 0.01, and the particles were considered as non-spherical. After obtaining an obscuration level of 12, 10 measurements were collected during 10 s while stirring. The parameters reported were D10, D50, D90, which are related to the volume-based particle size distribution for which 10, 50, and 90%, respectively, of the particles are smaller than this size. In addition, the volume moment mean diameter D [4,3] in which the proportion of particles for each size is weighted according to their volume when calculating the mean size were reported.

Statistical Analysis

The findings from particle size analysis were statistically evaluated with the two-way analysis of variance (**ANOVA**) option of the GLM procedure present in SAS software (SAS Institute, 1988). The main effects of meat abnormality coupled with the sampling position (NB superficial, NB deep, WB superficial, WB deep), the storage time, and their interactions were evaluated and means separated using the Tukey's HSD test (multiple range test) of the GLM procedure. In addition, correlations between the results from multi-angle light scattering, compression test, and shear force at each storage time were performed (SAS Institute, 1988).

RESULTS AND DISCUSSION

Macroscopic Observation and Histology

In the present study, the differences in the histological features observed between the superficial and the deep part of the WB fillets, reported for the first time in our previous study (Soglia et al., 2016), were further investigated. The WB muscles sampled after 10, 72 and 168 h post mortem were macroscopically hard and exhibited a transparent exudate and/or hemorrhages (petechiae or small hemorrhages) on the surface in agreement with Sihvo et al. (2014) and Trocino et al. (2015). On the contrary, the NB samples did not show any superficial lesions.

As to the microscopic observations, according to the PMF myodegeneration (Figure 2), the NB breasts were graded as F1 and F2 (2 samples) with the F1 samples (Figure 2A) exhibiting some abnormal fibers and

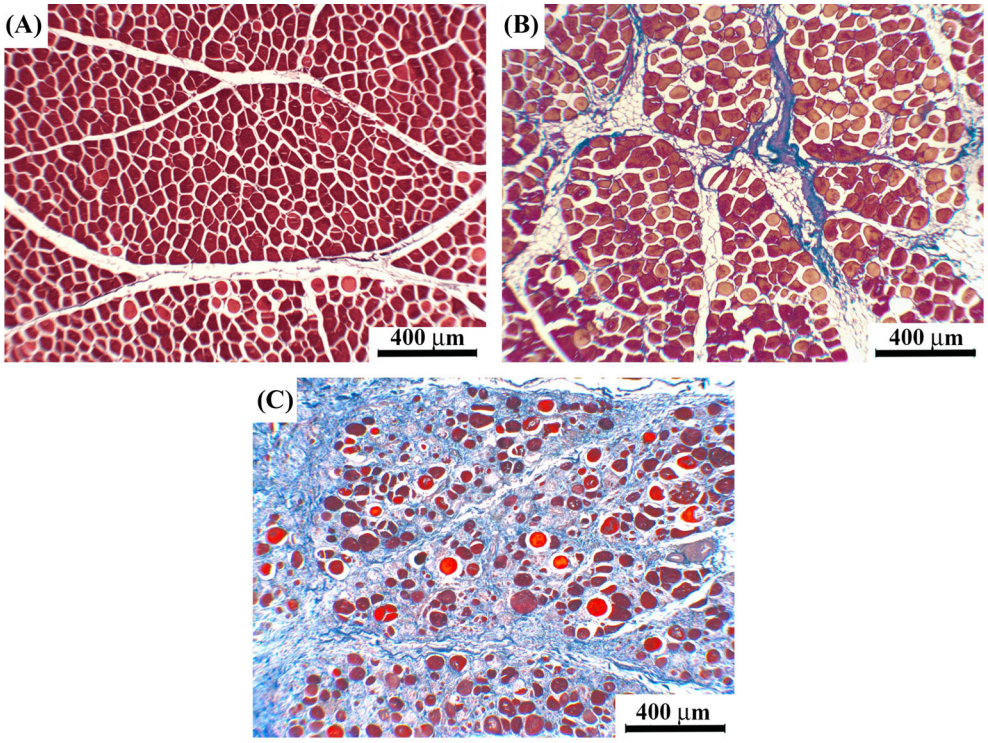

Figure 2. Histological representation of levels of myodegeneration. Score F1 – mild histogical changes: abnormal fibers ranging from 2 to 4 for each primary myofiber fascicle (PMF) (Figure 2A); Score F2 – moderate: abnormal fibers ranging from 5 to 10 for each PMF, and connective and fatty tissue infiltrates the perimysial space (Figure 2B); Score F3 – severe: abnormal fibers represent the majority of the fibers for each PMF, and the muscle fibers exhibit high variability in size. Muscle fibers are immersed in an abundant connective tissue (Figure 2C).

intermingled normal muscle fibers. The F2 muscles (Figure 2B) revealed an increased number of rounded fibers with characteristic hyalinization and nuclear internalization. On the other hand, the WB samples exhibited severe myodegeneration (F3, Figure 2C) and fibrosis both in the superficial and in the deep part. In addition, in agreement with previous studies, many histopathological features such as hyaline and vacuolar degeneration, necrosis and lysis and plentiful inflammatory infiltrate were observed (Sihvo et al., 2014; Trocino et al., 2015; de Brot et al., 2016; Soglia et al., 2016). No changes in the histological features were observed with storage time at 10, 72 and 168 h post mortem either in NB or WB samples.

The main causes and/or consequences associated with the increase of interstitial connective tissue (resulting in fibrosis) might be attributed to a reduced microcirculation and subsequent impaired muscle fiber metabolism and oxygen supply leading to ischemia (Sosnicki and Wilson, 1991; Kuttappan et al., 2013; Petracci et al., 2015; Trocino et al., 2015) and hypoxia (Hoving-Bolink et al., 2000; Joiner et al., 2014). In this regard, the WB cases exhibited a differential expression of the genes associated with hypoxia as assessed by Mutryn et al. (2015) through a RNA-sequencing analysis. In addition, although microischemia was previously linked to the reduced endomysial and perimysial spaces and capillary density (and capillary to fiber ratio) (Sosnicki and Wilson, 1991; Dransfield and Sosnicki, 1999; Velleman et al., 2003), the findings of the present study revealed an accumulation of endomysial and perimysial fibrotic tissue and a subsequent increase in the spaces between the muscle fibers. Similar histological features exhibiting endomysial fibrosis and an increase in capillary-to-myofiber distance were previously observed in *mdx* mice (Desguerre et al., 2009; Latroche et al., 2015). In addition, an increase in the inter-capillary distance and an impaired angiogenesis were respectively found in dystrophic 7- to 10-month-old golden retriever and *mdx* mice (Nguyen et al., 2005; Matskas et al., 2013). Thus, since the increase of connective tissue might be associated with a lower capillary density and a longer inter-capillary distance, fibrosis seems to be one of the main factors linked to the impairing of the microvascular architecture in dystrophic skeletal muscles. Thus, the physical barrier and/or distance between the capillary/microvessel contour and the myofiber, might contribute in explaining the different degree of myodegeneration observed in the superficial and the deep part of the *Pectoralis major* muscles affected by WB abnormality: being more distant from the blood vessels responsible for oxygen translocation, the superficial part is more severely affected.

Texture and Particle Size Analysis

Texture The peak forces recorded when compressing both the raw and the cooked meat samples by 40 and 80% of their initial height are shown in Table 1. With regard to raw meat, a similar trend was found in the

Table 1. Compression values in Newtons (N) measured on both raw and cooked samples excised from different sampling position (superficial or deep layer) for NB and WB fillets (n = 6 samples/group/storage time). The values were recorded after compressing the samples to 40% and 80% of their initial height following storage for 10, 24, 72, 120, and 168 h post mortem.

Compression	Group	Storage time (h) 10	24	72	120	168	SEM
Raw meat							
40% (N)	NB surface	6.9^{Y}	$8.8^{X,Y}$	$8.8^{X,Y}$	6.9	$8.8^{X,Y}$	0.9
	NB deep	6.9^{Y}	4.9^{Y}	6.9^{Y}	6.9	4.5^{Y}	0.9
	WB surface	27.5^{X}	20.6^{X}	22.6^{X}	18.6	22.6^{X}	1.9
	WB deep	11.8^{Y}	$10.8^{X,Y}$	$10.8^{X,Y}$	8.8	8.8^{Y}	0.9
80% (N)	NB surface	17.7^{Y}	$15.7^{X,Y}$	14.7	$14.7^{X,Y}$	17.7	0.9
	NB deep	15.7^{Y}	12.8^{Y}	14.7	$14.7^{X,Y}$	14.7	0.9
	WB surface	$32.4^{a,X}$	$24.5^{a,b,X}$	20.6^{b}	$24.5^{a,b,X}$	$21.6^{a,b}$	1.9
	WB deep	16.7^{Y}	12.8^{Y}	10.8	11.8^{Y}	11.8	0.9
Cooked meat							
40% (N)	NB surface	55.9^{a}	$44.1^{a,b}$	$33.4^{a,b}$	32.4^{b}	$36.3^{a,b}$	1.9
	NB deep	54.9	51.0	35.3	33.4	36.3	1.9
	WB surface	52.0	49.1	45.1	42.2	34.3	2.9
	WB deep	48.1	46.1	39.2	40.2	34.3	1.9
80% (N)	NB surface	$105.0^{a,X,Y}$	$69.7^{a,b}$	55.9^{b}	53.0^{b}	$57.9^{a,b}$	5.9
	NB deep	$131.5^{a,X}$	$95.2^{a,b}$	61.8^{b}	60.8^{b}	72.6^{b}	6.9
	WB surface	69.7^{Y}	67.7	56.9	54.0	51.0	2.9
	WB deep	$89.3^{X,Y}$	76.5	63.8	62.8	62.8	3.9

^{a,b}Mean values within the same row followed by different superscript letters significantly differ among the storage time ($P \leq 0.05$).
^{X,Y}Mean values within the same column followed by different superscript letters significantly differ within the compression groups; SEM = Standard error of mean.

values measured either at 40 or 80% of compression. In detail, considering the compression values measured 10 h post mortem, no significant differences were found between the deep layer of the WB cases and either the superficial or the deep layer of the NB. Notwithstanding, the superficial layer of the WB cases exhibited pronounced higher 40 and 80% compression values measured at the earliest sampling time of 10 h. Although the 40% compression measurements did not reveal any evolution in raw meat tenderness during storage, compression to 80% of the initial height showed that there is a tendency for a progressive softening process taking place within the superficial layer of the WB samples from 10 to 72 h post mortem. Increased compression values have been previously reported in the caudal portion of the *Pectoralis major* muscles affected by WB abnormality (Mudalal et al., 2015), but this study aims at evaluating the textural properties of meat keeping the superficial layer separated from the deep one.

Among the cooked samples, compression values (measured both at 40 and 80% of compression) did not differ among the groups, indicating that the shearing properties of cooked meat were not affected by WB, with the only exception being the samples at 10 h post mortem. In that case, the surface layer of the WB cases (both the superficial and the deep part) exhibited lower values than at other time points, measured at 80% compression. On the other hand, a progressive decrease in hardness was found to occur during post mortem storage of the NB samples. In agreement with cooked meat compression results, the intra-fillet sampling position did not exert any relevant effect on Allo-Kramer shear force. An overall progressive tenderization process took place during storage ($P \leq 0.001$) of NB and WB samples, the last ones exhibiting significantly higher ($P \leq 0.05$) shear force values (data not shown). The findings from texture analysis revealed that the differences between the WB vs. NB groups were mainly detected when raw meat rather than cooked was analyzed. This result might be partly explained considering the findings from the histological observation of the WB cases. Thus, the increase of interstitial connective tissue resulting in fibrosis (Sihvo et al., 2014), observed also in this study, and the increased deposition of extracellular matrix (glycosaminoglycans; Velleman and Clark, 2015) seen within the WB samples might exert a relevant effect on raw meat hardness. However, in spite of aforementioned increased amount of connective tissue components found in the WB cases, thermally labile cross-links may be the reason for the similar evolution of compression and shear force values measured on both WB and NB cooked samples. Heat denaturation/solubilization of collagen was thus found to occur readily at temperatures between 53 and 63°C (Martens et al., 1982).

Particle Size Analysis The typical shape of a particle size distribution curves for both NB and WB samples are shown in Figure 3. In their previous study, Lametsch et al. (2007) extracted myofibrillar protein from porcine *Longissimus dorsi* muscles and found a monomodal distribution curve that was related to the length of the myofibrils and their fragmentation products. In fact, the length of a purified myofibril was previously reported to be around 100 μm (Hopkins et al., 2000). In our study, the distribution curve exhibited a tri-modal shape likely because of the structural differences between the species and muscles and that no purification of the myofibrillar protein was performed before analyzing the particle size distribution of the samples. This protocol was followed according to Lametsch

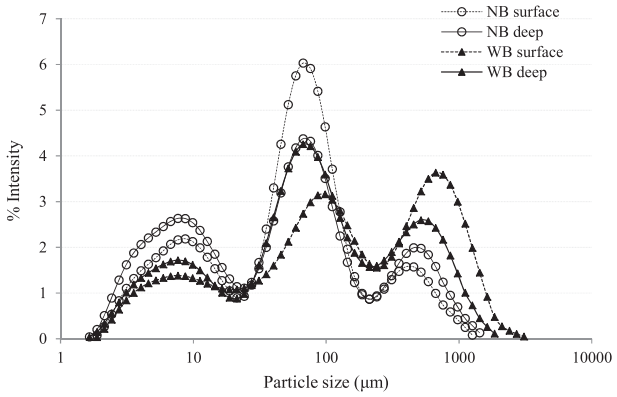

Figure 3. Example of a typical shape of the particle size distribution curves for both NB (round-shaped, open) and WB (triangle-shaped, solid black) samples considered as surface (dotted line) and deep (solid line) layer.

et al. (2007) who found that, when using multi-angle light scattering to estimate particle size, measurements can be performed on a meat homogenate and differences in the particle size distribution were more pronounced when a meat homogenate rather than partly purified myofibrils was analyzed. Moreover, following this procedure, a difference in the fragmentation pattern between NB and WB samples was observed. In comparison with NB, the WB cases exhibited a higher overall volume of the fraction of particles characterized by a larger size. This effect was more evident in the superficial part than in the deep layer of the WB muscles, as shown in Figure 4 where the evolution of the D10, D50 and D90 during refrigerated storage at 4 ± 1°C is reported. As shown in Figure 4A, no significant differences were found either in the superficial or the deep layer of the NB samples during a 7-d storage. On the other hand, both the superficial and the deep part of the WB cases exhibited remarkably higher ($P \leq 0.001$) D10, D50 and D90 indexes that significantly ($P \leq 0.001$) decreased following storage. The results concerning the evolution in D50 and D90 for both NB and WB samples are shown in Figure 4B and C. As to D50 (Figure 4B), a similar trend was observed for both the superficial and the deep layer of NB samples without any relevant variations caused by the storage time. On the other hand, after increasing up to d 3, an overall decrease in D50 was observed in the WB fillets at d 7 (both in the superficial and the deep part). A similar trend was observed in D90 and D [4:3] (Figure 4C and D) except for the deep layer of the WB samples that exhibited a particle size distribution comparable to those found in NB.

This increase in intermediate and large size particles observed in the WB samples (mainly the superficial layer) might be explained by considering the role

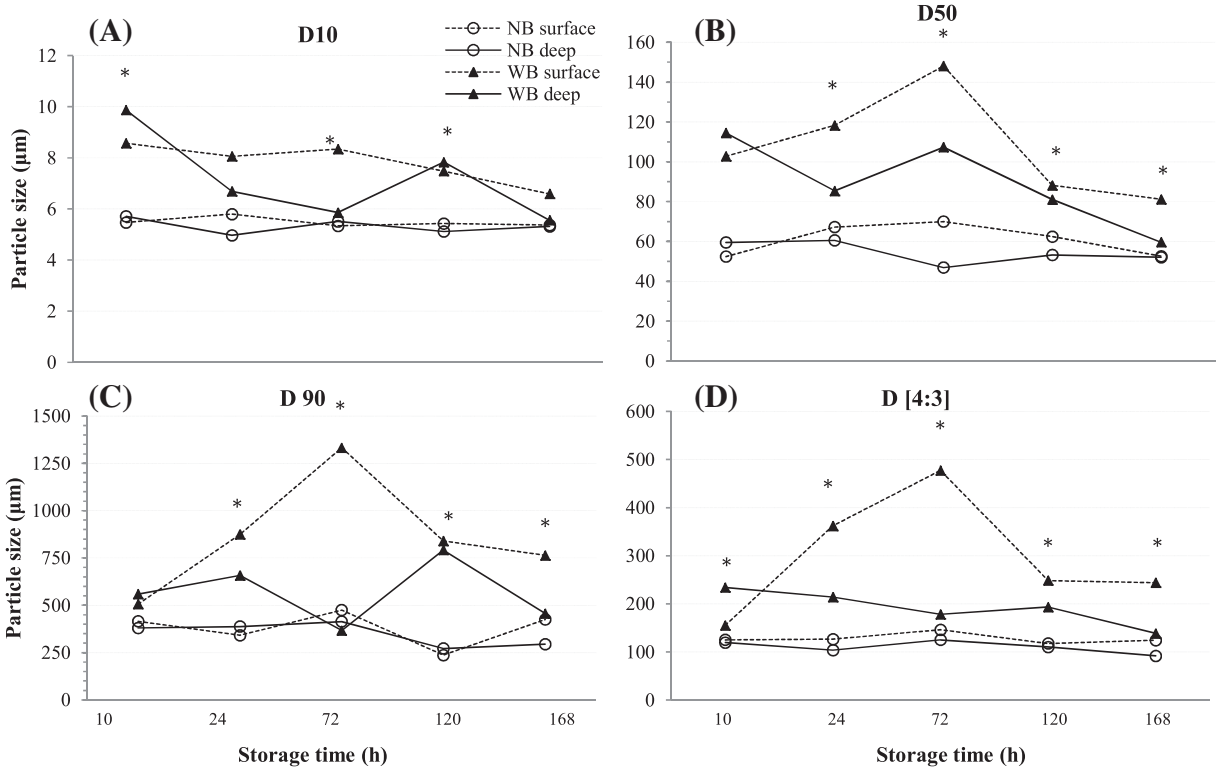

Figure 4. Results of the distribution parameters resulting from the multi-angle light scattering during 7 d of refrigerated storage for both normal (NB) (round-shaped, open) and wooden breast (WB) (triangle-shaped, solid black) samples considered as superficial (dotted line) and deep (solid line) layer (n = 30). The parameters D10 (Figure 4A), D50 (Figure 4B), D90 (Figure 4C) related to the particle size below which 10, 50, and 90% of the particle exist and D[4,3] (Figure 4D) in which the proportion of particles for each size is weighted according to their volume when calculating the mean size were considered in this study. * = Within each storage time mean values significantly differ ($P \leq 0.001$) among the experimental groups (NB surface, NB deep, WB surface, WB deep).

Table 2. Correlations between the distribution parameters D10, D50, D90, and D[4:3] resulting from multi-angle light scattering, compression test, and shear force.

					Compression raw		Compression cooked	
	D10	D50	D90	D[4:3]	40%	80%	40%	80%
D10								
D50	0.655***							
D90	0.497***	0,868***						
D[4:3]	0.561***	0.920***	0.987***					
Compression raw 40%	0.323**	0.447***	0.458***	0.466***				
Compression raw 80%	0.336**	0.449***	0.523***	0.527***	0.516***			
Compression cooked 40%	0.307*	0.223	0.196	0.213	− 0.191	0.078		
Compression cooked 80%	0.039	− 0.055	− 0.197	− 0.168	− 0.195	− 0.123	0.609***	
Shear force	0.050	− 0.043	− 0.128	− 0.118	− 0.058	0.101	0.327*	0.563***

*$P \leq 0.05$; ** $P \leq 0.01$; *** $P \leq 0.001$.

of the extracellular matrix in maintaining the skeletal muscle structure. As previously reported, an accumulation of interstitial connective tissue and diffuse thickening in the interstitial fraction and deposition of variable amounts of loose connective tissue (fibrosis) was widely found in the WB samples (Figure 2C). Such collagenous structures provide the connective tissue with a high degree of inherent strength which in turn contributes to resistance to shearing of the muscle tissue during homogenization. The larger particle size of WB muscles is likely a consequence of not only the connective tissue itself giving rise to larger particles, but also that it protects other structures, such as the myofibrils, against fragmentation during the homogenization. In agreement with our findings, Sihvo et al. (2014) observed a longitudinal fragmentation in degenerating fibers, but the results of this study indicate that the increase in connective tissue overcomes the longitudinal fragmentation in WB cases. Similarly, Feit and Domke (1982), demonstrated that the increased resistance to fragmentation observed in dystrophic chicken muscles might be attributed to an altered muscle structure. In addition to collagen, since the proteoglycans are another principal component of the extracellular matrix and are particularly stable at low temperatures, their accumulation around the skeletal muscle fibers and within the interstitial spaces (Serrano and Munoz-Canoves, 2010) might also be responsible for the larger fraction of larger particles and for the increase in particles with larger size found within the WB samples. On the other hand, the structures in the WB cases giving rise to the larger particles may have exhibited a degradation processes at the later stage of storage (from d 3 toward d 7), leading to muscle tissue fragmentation including softening of the connective tissue and subsequently resulting in an overall decrease in larger particles.

Correlations The correlations between the results from multi-angle light scattering, compression test and shear force are shown in Table 2. Significant correlations ($P \leq 0.001$) were found between all the distribution parameters obtained from multi-angle light scattering and the compression test (both 40 and 80% compression) assessed on raw meat. This suggests that the increased amount of connective tissue components observed in the WB samples provides a high degree of inherent strength which in turn result in modified textural properties and contribute to resistance of the muscle tissue during homogenization. On the other hand, no significant correlations were found between the distribution parameters and either the compression test or the shear force measured on cooked meat. This finding might be explained considering the thermally labile cross-links that can be speculated to be present in the newly deposed connective tissue found in WB. In detail, the heat-induced changes in the extracellular matrix (leading to denaturation of collagen and likely of proteoglycans) may be the reason for the analogous evolution in textural properties assessed after cooking the NB and WB samples.

CONCLUSIONS

The findings of the present study led to a deeper knowledge concerning the effect of the WB abnormality on the histological features, texture, and fragmentation pattern of meat during 7 d of storage. Considering the different degree of myodegeneration observed within the WB muscles, in the present study the superficial and the deep part of the *Pectoralis major* muscles were analyzed separately in order to investigate if the sampling position exerts a relevant role in determining the main features of the WB fillets. Although no changes in the histological features were found after 10, 72 and 168 h post mortem either in NB or WB samples, the latter exhibited severe myodegeneration accompanied by nuclear internalization, hyaline and vacuolar degeneration and accumulation of perimysial and endomysial connective tissue in both superficial and deep part. With regard to texture, the differences among the groups were mainly detected when raw meat rather than cooked was analyzed. The hardness of raw WB was mainly observed in the superficial part of the fillet. As to particle size analysis, the increase of connective tissue (extracellular matrix) and fibrosis might account for the different fragmentation pattern observed between the superficial and the deep layer in the WB cases, with the superficial part exhibiting a higher amount of larger particles and an increase in particles with larger size during storage.

REFERENCES

Campo, M. M., P. Santolaria, C. Sanudo, J. Lepetit, J. L. Olleta, B. Panea, and P. Alberti. 2000. Assessment of breed type and ageing time effects on beef meat quality using two different texture devices. Meat Sci. 55:371–378.

de Brot, S., S. Perez, H. L. Shivaprasad, K. Baiker, L. Polledo, M. Clark, and L. Grau-Roma. 2016. Wooden breast lesions in broiler chickens in the UK. Vet. Rec. 178:141.

Desguerre, I., M. Mayer, F. Leturcq, J. P. Barbet, R. K. Gherardi, and C. Christov. 2009. Endomysial fibrosis in Duchenne muscular dystrophy: a marker of poor outcome associated with macrophage alternative activation. J. Neuropathol. Exp. Neurol. 68:762–773.

Dransfield, E., and A. A. Sosnicki. 1999. Relationship between muscle growth and poultry meat quality. Poult. Sci. 78:743–746.

Feit, H., and R. Domke. 1982. Fragmentation analysis of normal and dystrophic avian muscle. Muscle Nerve 5:373–381.

Hopkins, D. L., P. J. Littlefield, and J. M. Thompson. 2000. A research note on the factor affecting the determination of myofibrillar fragmentation. Meat Sci. 56:19–22.

Hoving-Bolink, A. H., R. W. Kranen, R. E. Klont, C. L. Gerritsen, and K. H. de Greef. 2000. Fibre area and capillary supply in broiler breast muscle in relation to productivity and ascites. Meat Sci. 56:397–402.

Joiner, K. S., G. A. Hamlin, A. R. Lien, and S. F. Bilgili. 2014. Evaluation of capillary and myofiber density in the pectoralis major muscles of rapidly growing, high-yield broiler chickens during increased heat stress. Avian Dis. 58:377–382.

Karumendu, L. U., R. van de Ven, M. J. Kerr, M. Lanza, and D. L. Hopkins. 2009. Particle size analysis of lamb meat: Effect of homogenization speed, comparison with myofibrillar fragmentation index and its relationship with shear force. Meat Sci. 82:425–431.

Kuttappan, V. A., H. L. Shivaprasad, D. P. Shaw, B. A. Valentine, B. M. Hargis, F. D. Clark, S. R. McKee, and C. M. Owens. 2013. Pathological changes associated with white striping in broiler breast muscles. Poult. Sci. 92:331–338.

Latroche, C., B. Matot, A. Martins-Bach, D. Briand, B. Chazaud, C. Wary, P. G. Carlier, F. Chrétien, and G. Jouvion. 2015. Structural and functional alterations of skeletal muscle microvasculature in dystrophin-deficient mdx mice. Am. J. Pathol. 185:2482–2494.

Lametsch, R., J. C. Knudsen, P. Ertbjerg, N. Oksberg, and M. Therkildsen. 2007. Novel method for determination of myofibril fragmentation post-mortem. Meat Sci. 75:719–724.

Lepetit, J., and J. Culioli. 1994. Mechanical properties of meat. Meat Sci. 36:203–237.

Liu, J., M. Ruusunen, E. Puolanne, and P. Ertbjerg. 2014. Effect of pre-rigor temperature incubation on sarcoplasmic protein solubility, calpain activity and meat properties in porcine muscle. LWT – Food Sci. Technol. 5:483–489.

Malvern. 2015. A Basic Guide to Particle Characterization. Malvern Instruments Limited, Worcestershire, UK.

Martens, H., E. Stabursvik, and M. Martens. 1982. Texture and colour changes in meat during cooking related to thermal denaturation of muscle proteins. J. Texture Stud. 13: 291–309.

Matsakas, A., V. Yadav, S. Lorca, and V. Narkar. 2013. Muscle ERRγ mitigates Duchenne muscular dystrophy via metabolic and angiogenic reprogramming. FASEB J. 27:4004–4016.

Mazzoni, M., M. Petracci, A. Meluzzi, C. Cavani, P. Clavenzani, and F. Sirri. 2015. Relationship between pectoralis major muscle histology and quality traits of chicken meat. Poult. Sci. 94:123–130.

Mudalal, S., M. Lorenzi, F. Soglia, C. Cavani, and M. Petracci. 2015. Implications of white striping and wooden breast abnormalities on quality traits of raw and marinated chicken meat. Animal 9:728–734.

Mutryn, M. F., E. M. Brannick, W. Fu, W. R. Lee, and B. Abasht. 2015. Characterization of a novel chicken muscle disorder through differential gene expression and pathway analysis using RNA-sequencing. BMC Genomics 16:399.

Nguyen, F., L. Guigand, I. Goubault-Leroux, M. Wyers, and Y. Cherel. 2005. Microvessel density in muscles of dogs with golden retriever muscular dystrophy. Neuromuscul. Disord. 15:154–163.

Olson, D. G., F. C. Parrish, Jr., and M. H. Stromer. 1976. Myofibril fragmentation and shear resistance of three bovine muscles during post-mortem storage. J. Food Sci. 41:1036–1041.

Petracci, M., M. Bianchi, S. Mudalal, and C. Cavani. 2013. Functional ingredients for poultry meat products. Trends Food Sci. Tech. 33:27–39.

Petracci, M., S. Mudalal, F. Soglia, and C. Cavani. 2015. Meat quality in fast-growing broiler chickens. World. Poult. Sci. J. 71:363–374.

SAS Institute, Inc. 1988. SAS/STAT User's Guide, release 6.03. SAS Institute, Inc., Cary, NC.

Serrano, A. L., and P. Munoz-Canoves. 2010. Regulation and dysregulation of fibrosis in skeletal muscle. Exp. Cell. Res. 316:3050–3058.

Sihvo, H. K., K. Immonen, and E. Puolanne. 2014. Myodegeneration with fibrosis and regeneration in the pectoralis major muscle of broilers. Vet. Pathol. 51:619–623.

Sihvo, H. K., J. Lindé, N. Airas, K. Immonen, J. Valaja, and E. Puolanne. 2017. Wooden breast myodegeneration of *pectoralis major* muscle over the growth period in broilers. Vet. Pathol. 54:119–128.

Soglia, F., S. Mudalal, E. Babini, M. Di Nunzio, M. Mazzoni, F. Sirri, C. Cavani, and M. Petracci. 2016. Histology, composition, and quality traits of chicken Pectoralis major muscle affected by wooden breast abnormality. Poult. Sci. 95:651–659.

Sosnicki, A. A., and B. W. Wilson. 1991. Pathology of turkey skeletal muscle: implications for the poultry science. Food Struct. 10:317–326.

Taylor, R. G., G. H. Geesink, V. F. Thompson, M. Koohmaraie, and D. E. Goll. 1995. Is Z-disk degradation responsible for postmortem tenderization? J. Anim. Sci. 73:1351–1367.

Trocino, A., A. Piccirillo, M. Birolo, G. Radaelli, D. Bertotto, E. Filiou, M. Petracci, and G. Xiccato. 2015. Effect of genotype, gender and feed restriction on growth, meat quality and the occurrence of white striping and wooden breast in broiler chickens. Poult. Sci. 94:2996–3004.

Velleman, S. G., J. W. Anderson, C. S. Coy, and K. E. Nestor. 2003. Effect of selection for growth rate on muscle damage during turkey breast muscle development. Poult. Sci. 82:1069–1074.

Velleman, S. G. 2015. Relationship of Skeletal muscle development and growth to breast muscle myopathies: A review. Avian Dis. 59:525–531.

Velleman, S. G., and D. L. Clark. 2015. Histopathological and myogenic gene expression changes associated with wooden breast in broiler breast muscles. Avian Dis. 59:410–418.